Complexes of Thiomandelate and Captopril Mercaptocarboxylate Inhibitors to Metallo-β-lactamase by Polarizable Molecular Mechanics. Validation on Model Binding Sites by Quantum Chemistry

JENS ANTONY,[1] JEAN-PHILIP PIQUEMAL,[2] NOHAD GRESH[3]

[1]Freie Universität Berlin, FB Mathematik und Informatik, Institut für Mathematik II, AG Biocomputing, Arnimallee 2-6, D-14195 Berlin, Germany

[2]Laboratory of Structural Biology, National Institute of Environmental Health Sciences, P.O. Box 12233, Research Triangle Park, NC 27709

[3]Laboratoire de Pharmacochimie Moléculaire et Cellulaire, FRE 2718 CNRS, IFR Biomédicale, 45, Rue des Saints-Pères, 75006 Paris, France

Received 23 November 2004; Accepted 7 February 2005

DOI 10.1002/jcc.20245

Published online in Wiley InterScience (www.interscience.wiley.com).

Abstract: Using the polarizable molecular mechanics method SIBFA, we have performed a search for the most stable binding modes of D- and L-thiomandelate to a 104-residue model of the metallo-β-lactamase from *B. fragilis,* an enzyme involved in the acquired resistance of bacteria to antibiotics. Energy balances taking into account solvation effects computed with a continuum reaction field procedure indicated the D-isomer to be more stably bound than the L-one, conform to the experimental result. The most stably bound complex has the S^- ligand bridging monodentately the two Zn(II) cations and one carboxylate O^- H-bonded to the Asn193 side chain. We have validated the SIBFA energy results by performing additional SIBFA as well as quantum chemical (QC) calculations on small (88 atoms) model complexes extracted from the 104-residue complexes, which include the residues involved in inhibitor binding. Computations were done in parallel using uncorrelated (HF) as well as correlated (DFT, LMP2, MP2) computations, and the comparisons extended to corresponding captopril complexes (Antony et al., J Comput Chem 2002, 23, 1281). The magnitudes of the SIBFA intermolecular interaction energies were found to correctly reproduce their QC counterparts and their trends for a total of twenty complexes.

 J Comput Chem 26: 1131–1147, 2005

Key words: metallo-β-lactamase; mercaptocarboxylate inhibitors; polarizable molecular mechanics; quantum chemistry; validation

Introduction

Metallo-β-lactamases are zinc enzymes inactivating β-lactam antibiotics by hydrolyzing their endocyclic amide bond.[1,2] As a major source of bacterial resistance against these antibiotics, metallo-β-lactamases have continuously attracted the interest of molecular modellers: molecular dynamics simulations of the entire protein[3] and quantum chemical calculations of active site complexes[4] have been performed, starting from structural information provided by X-ray crystallography.[1,2,5–8] Frequently, experimental studies are complemented by molecular modeling of inhibitor docking.[5,9–14]

Because resistance to β-lactam antibiotics mediated by metallo-β-lactamases is an increasing problem, the study of inhibitors of metallo-β-lactamases is a very important task. We report on complexes of thiomandelic acid, a broad spectrum and reasonably potent inhibitor of metallo-β-lactamases.[15] Combination of ^{1}H, ^{15}N, and ^{113}Cd NMR, and ^{111m}Cd perturbed angular correlation (PAC) of γ-ray spectroscopies showed that the inhibitor thiol binds to both metal ions.[14] Molecular modeling of complexes between

Correspondence to: N. Gresh; e-mail: Nohad.gresh@univ-paris5.fr

Contract/grant sponsor: Ligue Nationale Contre le Cancer (Comité de Paris)

This article includes Supplementary Material available from the authors upon request or via the Internet at http://www.interscience.wiley.com/jpages/0192-8651/suppmat

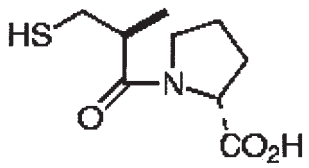

D-Captopril

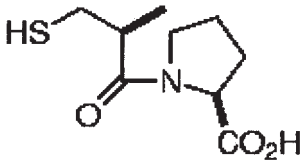

L-Captopril

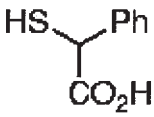

Thiomandelic acid

Chart 1. Representation of the structures of thiomandelate and captopril inhibitors.

thiomandelic acid and *B. cereus* metallo-β-lactamase using the AMBER force field additionally identified an interaction between one oxygen of the carboxylate group of the inhibitor and the NH_3^+ of Lys171. The other carboxylate oxygen atom interacts with the Zn(II) cation, which is coordinated by a cysteine, an aspartate, and a histidine ($Zn(II)^b$) for the D-isomer of the inhibitor, but not for L-thiomandelate.[14] Here we probe different binding modes of thiomandelic acid using polarizable molecular mechanics and compare to our previous results obtained for the inhibitor captopril.[16]

The structures of thiomandelate and captopril are represented in Chart 1. We will proceed similarly to our previous study devoted to the binding of D- and L-captopril to β-lactamase, which resorted to SIBFA and, for model binding sites, to parallel SIBFA and quantum chemistry (QC) calculations.[16] Thus, we first perform a search for the most favorable modes of binding by energy minimization (EM). The energy balances take into account the energy of the protein–inhibitor complex, the minimized energies of a model of uninhibited protein and of the isolated inhibitor, and the contribution of solvation using a Continuum procedure. The recognition site has eight amino acid residues. These are five neutral residues: His99, His101, His162, Asn193, His223; two anionic residues, Asp93 and Cy^-181, one cationic residue, Lys184, and two Zn(II) dictations at 3.5 Å from one another. The inhibitor has two candidate Zn(II)-binding moieties, thiolate and carboxylate, with only one C atom interposed in between, and has an aromatic ring. The vicinity of up to seven charged entities [the two Zn(II) cations, Asp103, Cy^-181, Lys184, and the thiolate and carboxylate groups of the inhibitor] results into very large nonadditivity effects of polarization, E_{pol}, and charge-transfer, E_{ct}, energy contributions. Such effects were seen in our previous study[16] to have different magnitudes, depending on the nature of the complexes. Their onset renders the use of conventional, nonpolarizable molecular mechanics problematic for energy comparisons between competing binding modes. This is further compounded by the issue of multipole transferability in constructing large molecules from constitutive fragments that was raised by Faerman and Price.[17] The need to compute simultaneously and consistently inter- and intramolecular E_{pol} and E_{ct} contributions has been underlined, and procedures have been developed towards this aim.[18,19] Thus, to validate our approach, we will extract from each energy-minimized β-lactamase complex, the terminal side-chain fragments of the above-mentioned residues, the inhibitor, and the two Zn(II) cations. For Asn193, the N-terminal part of the backbone and the entire side chain are extracted. Single-point SIBFA energy computations are performed, and, in parallel, uncorrelated and correlated QC computations with two different basis sets. We will also test a new formulation of the SIBFA first-order contributions. The same comparisons are also reported for captopril, thus totalling up to 20 complexes, and are extended to the computations of continuum solvation energies.

Procedure

Quantum Chemistry Computations

The *ab initio* computations used the Coreless Effective Potential (CEP) 4-31G(2d) basis set developed by Stevens et al.,[20] which encompasses two 3d polarization functions on the heavy atoms, and the LACV3P** basis set, which is equivalent to the 6-311G** set on the nonmetal atoms.[21] The contribution of correlation to the CEP 4-31G(2d) binding energy was evaluated using the MP2 procedure.[22] The DFT computations used the B3LYP[23] functional and the CEP 4-31G(2d) basis set as well as the LACV3P** basis set. The LMP2 computations are based on the approach developed by Saebo et al.,[24] and resorted to the LACV3P** basis set. The CEP 4-31G(2d) computations used the Gaussian 03[25] and the LACV3P** ones used the Jaguar 5.0 software.[26] The HF and LMP2 methods in Jaguar use a pseudospectral method to compute the integrals.[27] The calculations of the continuum solvation energies were done using the Poisson–Boltzmann equation within the HF as well as the DFT procedures.[28]

SIBFA Computations

The intermolecular interaction energy was computed as a sum of five components: electrostatic multipolar energy (E_{MTP}), short-range repulsion (E_{rep}), polarization (E_{pol}), charge transfer (E_{ct}), and dispersion (E_{disp}). The multipoles (up to quadrupoles) were distributed on the atoms and the bond barycenters using a procedure developed by Vigné–Maeder and Claverie.[29] The anisotropic polarizabilities were distributed on the centroids of the localized

orbitals (heteroatom lone pairs and bond barycenters) using a procedure due to Garmer and Stevens.[30] The expression of each contribution was detailed in our previous articles.[31] For the validation calculations of this work, we have also tested a new formulation of the two first-order contributions. Thus, E_{MTP} is augmented with a "penetration" component E_{pen}, which is most of the time attractive and mimics the effects of the overlap of the electron clouds of the interacting molecules. The expression for E_{pen} in SIBFA was given in ref. 32. E_{rep} is expressed as the sum of bond–bond, bond–lone pair, and lone pair–lone pair interactions. Denoting by R_{IJ}, the distance between the centroids of localized orbitals such as I and J (chemical bonds or lone pair hybrids), and by S a representation of the overlap between such interacting bonds and/or lone pairs, the S^2/R expression (see ref. 31) is now augmented with as an S^2/R^2 term, following an earlier proposal by Murrell and Teixeiras-Dias.[33] It was calibrated in a limited set of H-bonded and monoligated cation–ligand complexes (Piquemal et al.,[34] Gresh et al.[35]) so as to reproduce the corresponding values of the short-range repulsion contribution E_{exch} from energy decomposition, instead of the actual difference between ($E_c + E_{exch}$) and E_{MTP}.

Finally, for both approaches, we have recalibrated the Zn-specific parameters for E_{ct} and, concerning E_{pol}, the screening parameters of imidazole and methanethiolate.

E_{ct}

The recalibration of E_{ct} in the case of Zn(II) has been motivated by several comparisons with *ab initio* energy decomposition analyses using the Restricted Variational Space Analysis (RVS) procedure[36] on polycoordinated Zn(II) complexes.[37] These had shown E_{ct}(SIBFA) to have an overestimated anticooperative character with respect to that of its RVS counterpart, leading in some cases, particularly with anionic ligands, to underestimated values. We have accordingly modified four Zn-specific parameters of E_{ct}, as detailed in an accompanying paper (Gresh et al.[35]). Such parameters were selected to reproduce the values of E_{ct}(RVS) in the $[Zn(H_2O)_6]^{2+}$ complex, while giving similar E_{ct} values as the previous parameters in Zn-monoligated complexes. Tests were subsequently performed on diverse tetra- and pentacoordinated Zn(II) complexes, as in Zn-finger models and the active site of β-lactamase in the presence of a hydroxide and a water molecule. They showed E_{ct}(SIBFA) to correctly reproduce the trends from E_{ct}(RVS).

E_{pol}

In SIBFA the field polarizing a given molecule or molecular fragment is screened by a Gaussian function, which has a multiplicative factor E, and an exponent F, specific for that fragment and initially calibrated for it[31b] so that the radial variations of E_{pol}(SIBFA) match the corresponding ones of E_{pol}(RVS) in its complexes with Zn(II) as a probe. We have reported in an accompanying paper (Gresh et al.[35]) the updated E and F values for imidazole and methanethiolate ligands. Such values were found to give an equally good match to E_{pol}(RVS) as those originally derived in ref. 31b, and an improved nonadditive behavior of E_{pol}(SIBFA) in polyligated complexes. All other molecular fragments retained the same E and F values as in the original article.[31b] Additional details are given in the accompanying article. The quadrupole polarizability on Zn(II) was not included, on account of its negligible effect in diverse polyligated Zn(II) complexes, as computed in the latter article.

Calculation of solvation energies ΔG_{solv}

ΔG_{solv} was computed using the Langlet–Claverie (LC) procedure[38] interfaced in SIBFA.[39] It is formulated as a sum of electrostatic, polarization, repulsion, and cavitation contributions. It uses the same *ab initio* distributed multipoles as SIBFA, ensuring mutual consistency. The parameters used were the same as in ref. 40.

Construction of the Protein and of the Inhibitors

The protein is assembled with the standard library of its constitutive backbone and side-chain fragments, encompassing the internal coordinates and the distributed multipoles and polarizabilities. The 104-residue model is built out of the nine oligopeptide sequences: Tyr40–Glu47, Met51–Met57, Leu68–Gln76, Phe95–Leu108, Ala120–Pro136, Tyr156–Val169, Phe178–Trp202, Val220–Gly224, and Thr235–Val239. The hydroxide and water ligands that coordinate the Zn(II) in the absence of inhibitor are removed in its presence. This assumption is supported by an X-ray crystallography study of the IMP-1 β-lactamase with a mercaptocarboxylate inhibitor, showing the inhibitor to replace these two ligands.[6] Thiomandelate was built out from methanethiolate, formate, and benzene fragments. Captopril was built out of methanethiolate, formate, formamide, two methanes, and proline. Standard bond lengths and valence angles were used.

Treatment of Flexible Molecules

We have resorted to a procedure that was developed and tested in recent studies of Zn(II) finger oligopeptides,[41] pentahydrated Zn(II) and Mg(II) complexes of 5′-guanosine monophosphate,[40a] organometallic complexes of Cu(II),[40b] and conformational studies of eleven model alanine and glycine tetrapeptides.[18d] To compute E_{MTP}, the multipoles were redistributed at the junctions between fragments following the procedure of ref. 42. To compute E_{pol}, the multipoles of the interfragment junctional bonds were not redistributed, and the junctional H atoms were located on the C or N atoms, from whence they originate. This procedure prevents the fragments from acquiring a nonnet fractional charge because of the multipole redistribution. It also prevents any junctional atom or bond multipole from being at too short distances (<1 Å) from a polarizable center belonging to an adjacent fragment. The total interaction energy was computed as the sum of intra- and intermolecular interfragment interactions computed simultaneously. The values of SIBFA "intermolecular" interaction energies in the model binding sites were computed as the difference between such a summed energy and that of the ligand alone in the same geometry as in the corresponding complex. The intramolecular energy of the terminal end of each side chain in these models was zero, because each consists of one single fragment; that of Asn193 was also zero, because it was constructed from four nonmutually interacting fragments, and there are insignificant energy differences

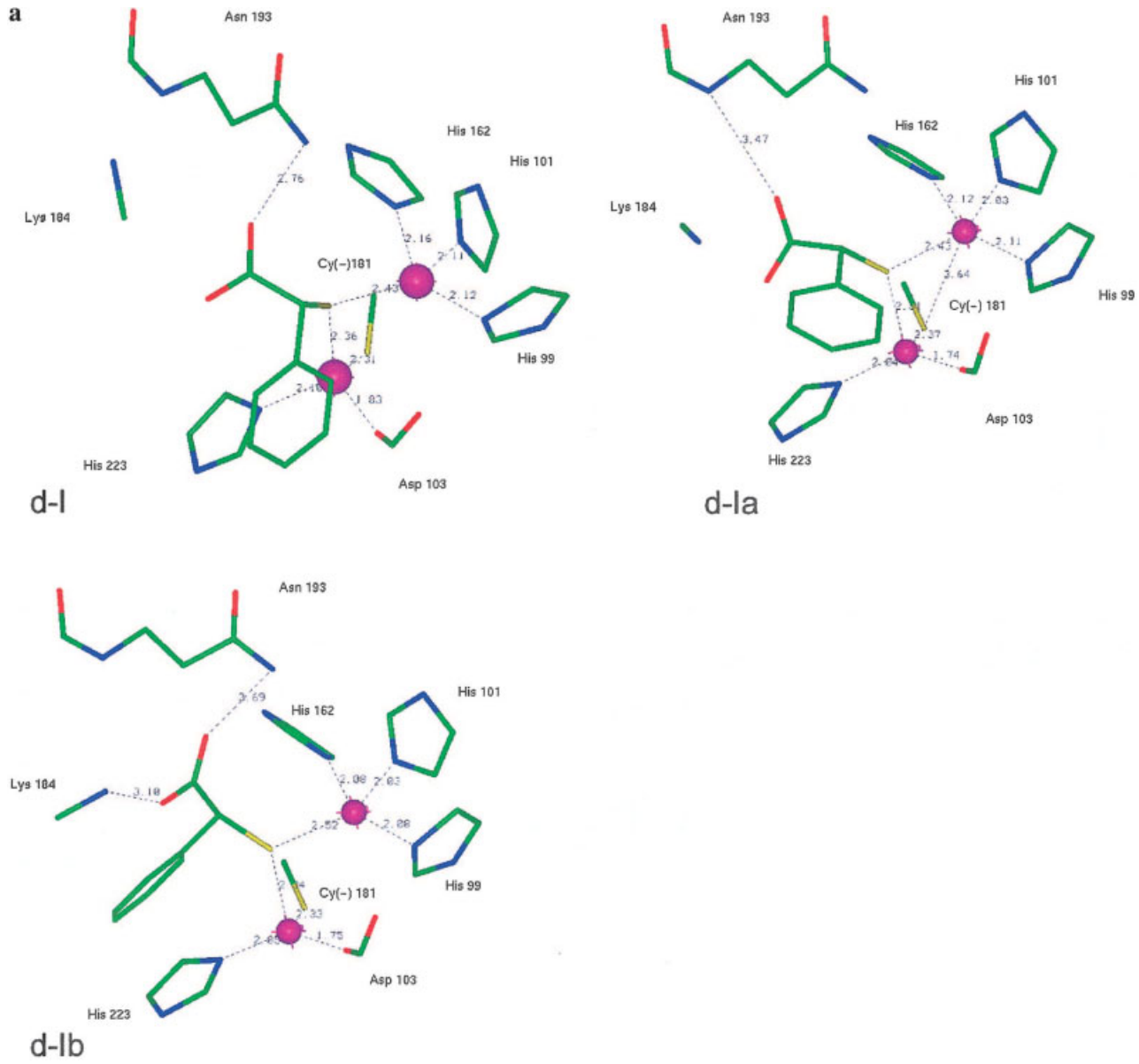

Figure 1. (a) Representation of complexes d-I, d-Ia, and d-Ib of thiomandelate with metallo-β-lactamase binding site. (b) Representation of complexes d-II, d-IIa, d-IIb, and d-III of thiomandelate with metallo-β-lactamase binding site. (c) Representation of complexes l-I, l-Ib, and l-III of thiomandelate with metallo-β-lactamase binding site. [Color figure can be viewed in the online issue, which is available at www.interscience.wiley.com.]

between the various Asn193 conformers, as confirmed by corresponding *ab initio* computations.

Energy Minimizations

These were done with the Merlin package.[43] As in ref. 16, the protein backbone was held rigid, and the side chains of eight residues in the recognition site were relaxed. The six intermolecular variables defining the inhibitor orientation in its complexes and its torsion angles were relaxed, as well as the positions of the two Zn(II) cations. We have resorted to the following strategy. The inhibitor was placed in the binding pocket of β-lactamase in the orientation with the lowest binding energy found with the Cff91 force field.[44] The orientation and conformation of the inhibitor were then minimized in the rigid enzyme, and subsequently together with relaxing the intramolecular degrees of freedom of the binding site. In the resulting complexes, no other coordination of the two Zn(II) cations by the inhibitor was found except by the bridging sulphur. Zinc coordination by the carboxylic acid of the inhibitor was enforced by introducing harmonic restraints between one of its oxygen atoms and one Zn(II) cation. Zinc coordination by the inhibitor's sulphur was assured by a second restraint between sulphur and the other Zn(II). After having prepared the

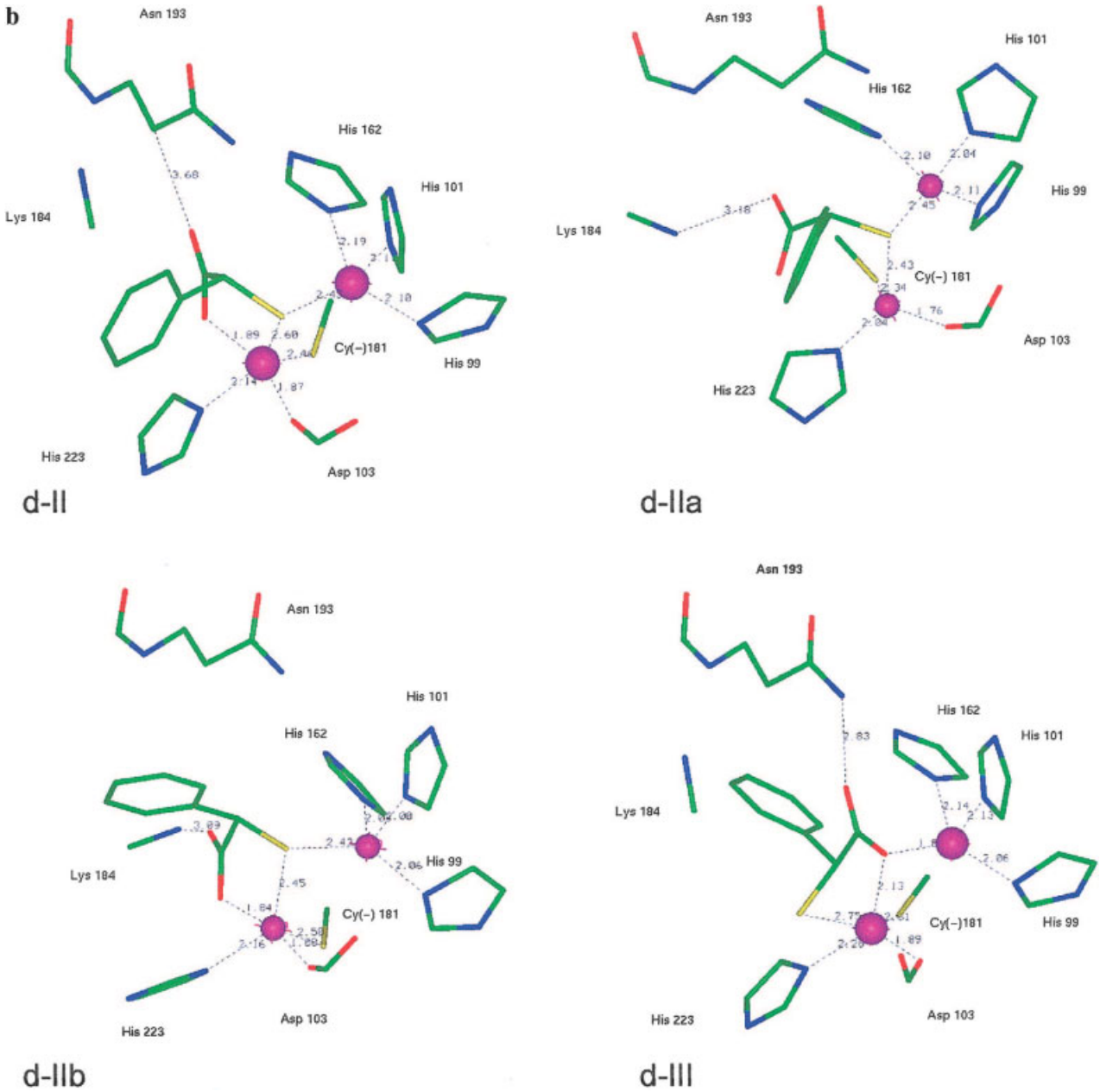

Figure 1. (*continued*)

inhibitor in the desired orientation, the restraints were removed and the structures were optimized as above, that is, first in the rigid and then in the flexible binding site.

Results and Discussions

104-Residue β-Lactamase

Three energy-minimized conformations were initially derived for both D- and L-isomers of thiomandelate. They are denoted as d-I to d-III and l-I to l-III for the respective isomers. However, none was characterized by a simultaneous binding of the carboxylate group to one Zn(II) cation through one O atom, and, through its second O atom, to the Lys184 side chain, as in the model recently proposed by Damblon et al.[14] Thus, to obtain such a model in our approach, we performed two constrained energy minimizations, using complexes d-I, d-II, and l-I as starting points. These complexes were the most likely ones to give rise to such a simultaneous interaction. For complexes d-Ia and d-IIa, a distance restraint (2.7 Å) was imposed between one carboxylate oxygen and

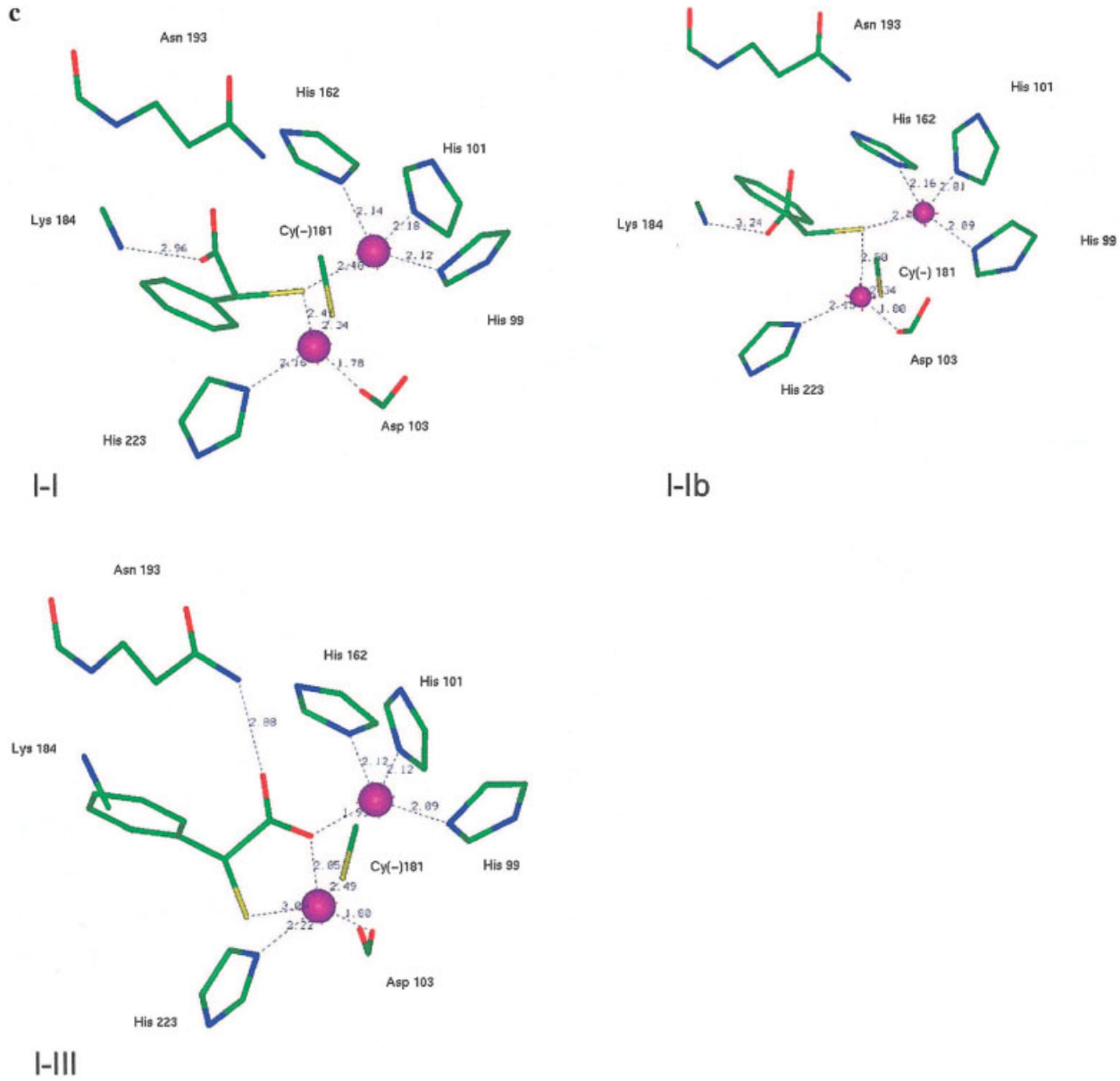

Figure 1. (*continued*)

the N atom of the Lys side chain. In complexes d-Ib, d-IIb, and l-Ib, an additional restraint (2.1 Å) was set between the other carboxylate O^- and the His223 bound Zn(II) cation, denoted as Zn(II)[b]. The structures derived by restrained energy minimization were postprocessed by a second round of energy minimizations with the distance restraints removed. A total of 11 complexes was thus derived from energy minimization. d-I, d-Ia, and d-Ib are represented in Figure 1a, d-II, d-IIa, d-IIb, and d-III in Figure 1b, and l-I, l-Ib, and l-III in Figure 1c. Complex l-II, with a very strong overlap with l-I (the heavy-atom rms is 0.4 Å) is not shown. The representation is limited to the inhibitor, the two Zn(II) cations, the terminal fragments of the side chains of residues His99, His101, Asp103, Cy^-181, Asn193, Lys184, and His223, as well as the N-terminal part of the Asn193 main chain. All complexes have closely comparable Zn coordination to the β-lactamase ligands: His99, His101, and His162 for the first and Asp103, Cy^-181, and His223 for the second, Zn(II)[b]. We describe below the more specific features of each.

D-thiomandelate

Complexes d-I, d-Ia, and d-Ib are "monodentate" ones, that is, only the S^- atom binds both Zn(II) cations. In d-Ib, the O^--Zn coordination was lost after removal of the distance restraints. In d-I, one carboxylate O^- is H-bonded to the Asn193 side chain. In d-Ia, this O^- is H-bonded to the Asn main chain. In d-Ib, the carbox-

Table 1. Energy Balances (kcal/mol) for the Complexes of D- and L-Thiomandelate with a 104-Residue Model of β-Lactamase.

	D-thiomandelate							L-thiomandelate				
	d-I	d-Ia	d-Ib	d-II	d-IIa	d-IIb	d-III	l-I	l-Ib	l-II	l-III	Uninhibited
E_{MTP}	−1802.6	−1826.9	−1849.9	−1865.1	−1879.6	−1923.8	−1806.8	−1821.4	−1825.2	−1814.5	−1773.3	−1852.0
E_{rep}	635.7	641.6	688.2	624.9	670.9	670.1	590.8	620.9	619.1	611.8	584.2	562.8
$\boldsymbol{E_l}$	**−1166.9**	**−1185.3**	**−1161.8**	**−1240.2**	**−1208.7**	**−1253.7**	**−1216.0**	**−1200.4**	**−1206.1**	**−1202.7**	**−1189.1**	**−1289.1**
E_{pol}	−422.0	−388.4	−395.6	−362.1	−370.9	−346.0	−396.4	−398.1	−388.7	−398.0	−410.1	−421.8
E_{ct}	−134.6	−150.0	−150.0	−112.1	−140.4	−116.2	−126.6	−131.1	−143.1	−131.6	−128.4	−100.9
E_{disp}	−373.6	−370.9	−384.6	−367.4	−379.5	−374.8	−350.7	−364.3	−364.5	−361.5	−348.1	−318.4
$\boldsymbol{E_{tot}}$	**−2097.0**	**−2094.6**	**−2091.9**	**−2081.6**	**−2099.4**	**−2090.6**	**−2089.7**	**−2093.9**	**−2102.4**	**−2093.7**	**−2075.7**	**−2131.5**
$\boldsymbol{E_{solv}}$	**−1645.8**	**−1636.1**	**−1618.3**	**−1621.8**	**−1609.3**	**−1607.4**	**−1643.7**	**−1622.8**	**−1622.8**	**−1621.8**	**−1646.3**	**−1550.3**
$\boldsymbol{\delta E = E_{tot} + E_{solv} - E_{lig0} + \delta E_{solv}}$	**−3584.9**	**−3572.8**	**−3552.3**	**−3545.5**	**−3550.8**	**−3540.1**	**−3575.5**	**−3558.8**	**−3567.3**	**−3557.6**	**−3564.1**	**−3586.0**
$\boldsymbol{\delta E_{fin} = \delta E - \delta E}$ **(uninhibited)**	**1.1**	**13.2**	**33.7**	**41.5**	**35.2**	**46.1**	**10.5**	**27.2**	**18.7**	**28.4**	**21.9**	

The balances are computed with respect to a β-lactamase model in which the inhibitor is replaced by Zn-ligating hydroxy and water. E_{lig0} denotes the intramolecular energy of isolated thiomandelate following energy minimization taking into account its continuum solvation energy. ΔG_{solv} is its continuum solvation energy in the energy-minimized conformation, and $\delta E_{solv} = -\Delta G_{solv}$. The values of E_{lig0} and δE_{solv} are 68.9 and 226.8 kcal/mol, respectively. The summed δE_{solv} value for hydroxy and water is 95.8 kcal/mol. δE(uninhibited) denotes the sum $E_{tot} + E_{solv} + \delta E_{solv}$ of β-lactamase in which thiomandelate is replaced by water and hydroxyl.

ylate is bound simultaneously through one O^- to the Lys184 side chain, and through the other to the Asn N side chain. Complexes d-II and d-IIb are "bidentate" ones. They are stabilized by the involvement of one O^- to the binding to $Zn(II)^b$ cation while the S^- remains bound in the Zn bridging position. In d-IIb, one O^- is H-bonded to the Lys184 side chain. This complex corresponds to the one proposed by Damblon et al.[14] In d-IIa, while the other O^- is H-bonded to the Lys184 side chain, the previous O^- is now remote from $Zn(II)^b$ (dO-Zn = 3.1 Å). d-III is also a bidentate complex, but it is now one O^- that bridges the two Zn(II) cations, S^- being bound to $Zn(II)^b$, and the other O^- being H-bonded to the Asn193 side chain.

L-thiomandelate

Complexes l-I and l-II are monodentate, S^- bridging the two Zn(II) cations, and one carboxylate O^- being H-bonded to the Lys184 side chain. Complex l-Ib has similar features as l-I. It was thus not possible with the present protocol to have a simultaneous binding of the carboxylate group to Lys and $Zn(II)^b$ in accordance with ref. 14. In complex l-III, similar to d-III, one O^- has displaced S^- from the Zn bridging position, while the other O^- is H-bonded to the Asn193 side chain.

Table 1 reports the energy balances for the 11 complexes of thiomandelate with the 104-residue β-lactamase model. We also report the corresponding energies for a model of inhibitor-free β-lactamase, in which the recognition site has the Zn(II) cations complexed by a water and a hydroxide ligand as in the X-ray crystal structure.[5] In this table, E_{tot} denotes the total energies of each complex and their individual contributions, namely: E_{MTP}, E_{rep}, and their sum, E_l, E_{pol}, E_{ct}, and E_{disp}. E_{tot} thus includes the energy of thiomandelate in the conformation it adopts in the corresponding complex. It also reports the value of the solvation energy E_{solv} using the Langlet–Claverie continuum reaction field procedure,[38] the value, E_{lig0}, of thiomandelate in its lowest energy-minimized conformation, and the value of thiomandelate solvation energy in this conformation. The latter, denoted as δE_{solv}, represents the desolvation energy cost for transferring thiomandelate from solution to the β-lactamase binding site. In the case of uninhibited β-lactamase, δE_{solv} corresponds to the summed continuum solvation energies of hydroxide and water. δE is the sum of E_{tot}, E_{solv}, E_{lig0}, and δE_{solv}. δE_{fin} is the difference, for each thiomandelate complex, between its δE value and that of uninhibited β-lactamase taken as energy zero. Table 1 shows d-I to be the most stable complex (δE_{fin} = 1.1 kcal/mol), with D-thiomandelate bridging monodentately through its S^- atom the two Zn(II) cations, and H-bonded through one carboxylate O^- to the Asn193 side chain. The next two complexes on the energy scale are d-III (δE_{fin} = 10.5 kcal/mol), in which it is one carboxylate O^- that occupies the Zn bridging position, and dIa (δE_{fin} = 13.2 kcal/mol), with S^- monodentately bridging the two Zn cations, and one carboxylate O^- H-bonded to the Asn N main chain. The most stable L-thiomandelate complexes are l-Ib (δE_{fin} = 18.7 kcal/mol), having a monodentate Zn binding by S^- and one O^- in a salt bridge with Lys184, and l-III (δE_{fin} = 21.9 kcal/mol) with one O^- replacing S^- in the Zn bridging position. Examination of Table 1 shows E_{solv} to play an essential role in the ranking of δE values. Thus, while l-Ib has the lowest E_{tot} value (−2102.4 kcal/mol), it is destabilized by 23 kcal/mol with respect to d-I by the E_{solv} term. The complexes with the least favorable E_{solv} values have a salt bridge between the Lys184 side chain and one O^-, namely: d-Ib, d-IIa, d-IIb, l-I, l-Ib, and l-II. A detailed discussion of the trends in individual contributions is resumed in Supporting Information S1.

Table 2. Complexes of D- and L-Thiomandelate with the Two Zn(II) Cations and the Eight Fragments Modeling the β-Lactamase Binding Site.

	d-I	d-Ia	d-Ib	d-II	d-IIa	d-IIb	d-III	l-I	l-Ib	l-II	l-III
LACV3P** basis set											
ΔE(HF)[a]	**−1229.5**	**−1249.3**	**−1244.5**	**−1249.0**	**−1257.2**	**−1262.5**	**−1245.8**	**−1276.6**	**−1262.3**	**−1275.6**	**−1233.8**
$\delta\Delta E$	47.1	27.3	32.1	27.6	19.4	14.1	30.8	0.0	14.3	1.0	42.8
CEP 4-31G(2d) basis set											
ΔE(HF)[b]	**−1270.8**	**−1288.7**	**−1282.5**	**−1287.5**	**−1296.3**	**−1299.7**	**−1276.9**	**−1313.9**	**−1297.8**	**−1312.6**	**−1266.9**
$\delta\Delta E$	43.1	25.2	31.4	26.4	17.6	14.2	37.0	0.0	16.1	1.3	47.0
ΔE(SIBFA)	**−1234.3**	**−1245.6**	**−1236.7**	**−1261.7**	**−1250.1**	**−1272.9**	**−1251.8**	**−1276.1**	**−1266.4**	**−1276.8**	**−1238.1**
$\delta\Delta E$	41.8	30.5	39.4	14.4	26.0	3.2	24.3	0.0	9.7	−1.5	38.0
ΔE(SIBFA*)	**−1251.8**	**−1262.9**	**−1254.1**	**−1275.2**	**−1264.7**	**−1280.5**	**−1264.9**	**−1295.6**	**−1283.1**	**−1295.4**	**−1250.7**
$\delta\Delta E$*	43.8	32.7	41.5	20.4	30.9	15.1	30.7	0.0	12.5	0.2	44.9
$\delta(\Delta E)$: SIBFA*/HF[a]	−22.3	−13.6	−9.6	−26.2	−7.5	−18.0	−19.1	−19.0	−20.8	−19.8	−16.9
$\delta(\Delta E)$: SIBFA*/HF[b]	19.0	25.8	28.4	12.3	31.6	19.2	12.0	18.3	14.7	17.2	16.2
δE_{thi}(HF)[a]	0.0	4.2	1.0	3.8	1.2	4.8	4.9	4.4	3.5	4.4	4.1
δE_{thi}(HF)[b]	0.0	2.5	1.0	2.2	1.3	6.5	2.9	2.6	2.5	2.6	3.6
δE_{thi}(SIBFA*)	0.0	6.0	1.9	6.8	2.0	18.2	5.7	6.2	6.7	6.2	7.9
δE(HF[a])	42.9	27.4	29.1	27.0	16.4	19.2	31.5	0.0	14.8	1.0	42.9
δE(HF[b])	40.6	25.1	29.8	26.0	16.3	18.1	37.4	0.0	13.9	1.3	48.1
δE(SIBFA*)	37.6	32.4	37.1	21.0	26.8	27.1	30.1	0.0	13.0	0.2	46.6

Values (kcal/mol) of the intermolecular interaction energies. Uncorrelated calculations and SIBFA ΔE values without the dispersion contribution.
[a]LACV3P** basis set.
[b]CEP(4-31G(2d)) basis set.

Nine out of the 11 complexes have E_{tot} values differing from one another by <13 kcal/mol. The small E_{tot} differences can result from large differences at the level of the individual contributions, with large preferences in terms of E_l (as for d-II, d-IIb) compensated by opposing preferences in terms of E_{pol} and/or E_{ct}, and, to a somewhat lesser extent, E_{disp}. d-I is observed to have a δE value differing only marginally (1 kcal/mol out of 3585) from δE in the uninhibited complex. However, this could be fortuitous, because of the choice of the nature of that complex as chosen to translate the energy zero, and it is the relative δE_{fin} values along the series that represent the quantities of interest. In the case of D-captopril, the δE_{fin} value for the most stable complex amounted to 14.9 kcal/mol.[16] This should be not taken as an indication for a more favorable thiomandelate than captopril affinity to β-lactamase, because the ΔG_{solv} computations in ref. 16 used a different calibration than the present one, slightly different Gaussian screening parameters for imidazole, a different calibration of Zn-specific parameters for E_{ct}, and different imidazole and thiolate screening factors in the expression of E_{pol}.

Validation of SIBFA Results

Thiomandelate

It was essential to evaluate the accuracy of the present computations by explicit comparisons with quantum chemistry computations. Although these can obviously not be undertaken on the 104-residue β-lactamase, they are tractable on the model binding sites described in Figures 1a–c, because of their limited size (88 atoms). Similar to our previous study bearing on the β-lactamase complexes with D- and L-captopril,[16] we have performed single-point SIBFA energy computations and, in parallel, uncorrelated and correlated (DFT, LMP2, MP2) QC computations with two different basis sets, LACV3P** and CEP 4-31G(2d), denoted as basis sets a and b, respectively.

Concerning the SIBFA calculations, in addition to the standard formulation used in the 104-residue model, we have tested a recently introduced refinement of the two E_l contributions, E_{MTP} and E_{rep}. These consisted in: (a) the explicit introduction of a "penetration" term, E_{pen}, to the multipolar contribution E_{MTP};[32] and (b) the recalibration of E_{rep} to fit the exchange contribution from energy decomposition in model H-bonded (Piquemal et al., unpublished) and monoligated Zn complexes (Gresh et al.[35]) instead of the difference between E_l(QC) and E_{MTP}. E_{rep} is, furthermore, formulated as the sum of an S^2/R term augmented with an S^2/R^2 term. Such a reformulated potential could not be used, however, in the 104-residue computations, because it is necessary to further extensively test it in computations on large oligopeptides.

We have reported in Tables 2 and 3 the results of the comparisons done at uncorrelated and correlated levels, respectively. Table 2 lists: the values of the HF intermolecular interaction energies, ΔE(HF), and the differences, $\delta\Delta E$, in ΔE(HF) values with respect to the best-bound complex taken as energy zero; the corresponding values of the SIBFA intermolecular interaction energies, ΔE(SIBFA), prior to including the dispersion contribution E_{disp}. The values with the new formulation are indicated with an *; the differences, $\delta\Delta E$, in ΔE(SIBFA) values

Table 3. Complexes of D- and L-Thiomandelate with the Two Zn(II) Cations and the Eight Fragments Modeling the β-Lactamase Binding Site.

	d-I	d-Ia	d-Ib	d-II	d-IIa	d-IIb	d-III	l-I	l-Ib	l-II	l-III
LACV3P** basis set											
ΔE(DFT)	−1281.6	−1298.9	−1299.7	−1301.8	−1310.3	−1316.0	−1293.1	−1328.8	−1314.1	−1328.3	−1284.1
ΔE(LMP2)	−1272.7	−1291.3	−1290.1	−1295.2	−1301.5	−1305.5	−1281.1	−1321.1	−1306.1	−1320.7	−1271.9
CEP4-31G(2d) basis set											
ΔE(DFT)	**−1369.0**	**−1385.3**	**−1384.4**	**−1384.0**	**−1395.5**	**−1391.9**	**−1365.0**	**−1410.8**	**−1395.4**	**−1409.7**	**−1357.3**
$\delta\Delta E$	41.8	25.5	26.4	26.8	15.3	18.9	45.8	0.0	15.4	1.1	53.5
ΔE(MP2)	**−1414.9**	**−1436.7**	**−1447.8**	**−1436.2**	**−1453.4**	**−1453.8**	**−1414.7**	**−1459.7**	**−1446.4**	**−1460.0**	**−1408.1**
$\delta\Delta E$	44.8	23.0	11.9	23.5	6.3	5.9	45.0	0.0	13.3	−0.3	51.6
ΔE_{tot}(SIBFA)	**−1358.1**	**−1378.6**	**−1376.6**	**−1387.0**	**−1385.6**	**−1408.6**	**−1362.0**	**−1400.6**	**−1390.7**	**−1399.1**	**−1350.2**
$\delta\Delta E_{tot}$	42.5	22.0	24.0	13.6	15.0	−8.0	38.4	0.0	9.9	1.5	50.4
ΔE_{tot}(SIBFA*)	**−1386.8**	**−1410.8**	**−1407.3**	**−1410.3**	**−1411.0**	**−1426.1**	**−1380.5**	**−1430.1**	**−1417.7**	**−1427.6**	**−1368.1**
$\delta\Delta E_{tot}$*	43.3	19.3	22.8	19.8	19.1	4.0	49.6	0.0	12.4	2.5	62.0
$\delta(\Delta E)$:SIBFA*/DFT[b]	−17.8	−25.5	−22.9	−26.3	−15.5	−34.2	−15.5	−19.3	−22.3	−17.9	−10.8
$\delta(\Delta E)$:SIBFA*/MP2[b]	28.1	25.9	40.5	25.9	42.4	27.7	34.2	29.6	28.7	32.4	40.0

Values (kcal/mol) of the intermolecular interaction energies. Correlated calculations and SIBFA ΔE values with the dispersion contribution.
[a]LACV3P** basis set.
[b]CEP(4-31G(2d)) basis set.

with respect to that in complex l-I taken as energy zero; the differences, $\delta(\Delta E)$:SIBFA*/HF, of ΔE(SIBFA*) values with respect to the corresponding HF ones; the differences, δE_{thi}, in conformational energies of thiomandelate with respect to its most stable conformation in the considered complexes, namely d-I, as computed from the various approaches; and the differences, δE, in stability of the complexes (which include the thiomandelate conformational energy variations) with respect to the energy of the most stable complex l-I. Table 3 gives the values of the correlated DFT, LMP2, and MP2 intermolecular interaction energies and corresponding SIBFA energies after inclusion of E_{disp} contribution, denoted as ΔE_{tot}(SIBFA); the differences, $\delta\Delta E$, of ΔE_{int} values with respect to its value in complex l-I, and the differences, $\delta(\Delta E)$:SIBFA*/DFT and $\delta(\Delta E)$:SIBFA*/MP2 in SIBFA vs. DFT and MP2 interaction energies as computed with basis set b. For conciseness, we did not report for the latter the comparisons with basis set a, because the trends are similar.

Uncorrelated Computations

Table 2 shows that the trends of ΔE(HF) are overall correctly reproduced by ΔE(SIBFA) and ΔE(SIBFA*). The latter values are consistently larger in magnitude (by 8 to 20 kcal/mol out of 1250) than the former, and therefore closer to the $\Delta E(HF)^b$ values, which use the same basis set [CEP(4-31G(2d)] as for the derivation of the SIBFA multipoles. ΔE(SIBFA*) has values consistently intermediate between the $\Delta E(HF)^a$ and the $\Delta E(HF)^b$ ones. It is underestimated with respect to $\Delta E(HF)^b$ by values in the range 12–32 kcal/mol out of 1250, corresponding to relative errors in a 1–3% range. It is overestimated with respect to $\Delta E(HF)^a$ by values in the range 8–26 kcal/mol out of 1230, that is, relative errors in the 0.5–2% range. The energy ranking of the 11 complexes is as follows:

$$\delta\Delta E(HF)^a$$

$$\begin{matrix}\text{l-I}\\0.0\end{matrix} \geq \begin{matrix}\text{l-II}\\1.0\end{matrix} > \begin{matrix}\text{d-IIb}\\14.1\end{matrix} \approx \begin{matrix}\text{l-Ib}\\14.3\end{matrix} > \begin{matrix}\text{d-IIa}\\19.4\end{matrix} > \begin{matrix}\text{d-Ia}\\27.3\end{matrix} \approx \begin{matrix}\text{d-II}\\27.6\end{matrix} > \begin{matrix}\text{d-III}\\30.8\end{matrix} \geq \begin{matrix}\text{d-Ib}\\32.1\end{matrix} > \begin{matrix}\text{l-III}\\42.8\end{matrix} > \begin{matrix}\text{d-I}\\47.1\end{matrix}$$

$$\delta\Delta E(HF)^b$$

$$\begin{matrix}\text{l-I}\\0.0\end{matrix} \geq \begin{matrix}\text{l-II}\\1.3\end{matrix} > \begin{matrix}\text{d-IIb}\\14.2\end{matrix} > \begin{matrix}\text{l-Ib}\\16.1\end{matrix} > \begin{matrix}\text{d-IIa}\\17.6\end{matrix} > \begin{matrix}\text{d-Ia}\\25.2\end{matrix} \geq \begin{matrix}\text{d-II}\\26.4\end{matrix} > \begin{matrix}\text{d-Ib}\\31.4\end{matrix} > \begin{matrix}\text{d-III}\\37.0\end{matrix} > \begin{matrix}\text{d-I}\\43.1\end{matrix} > \begin{matrix}\text{l-III}\\47.0\end{matrix}$$

$$\delta\Delta E(\text{SIBFA*})$$

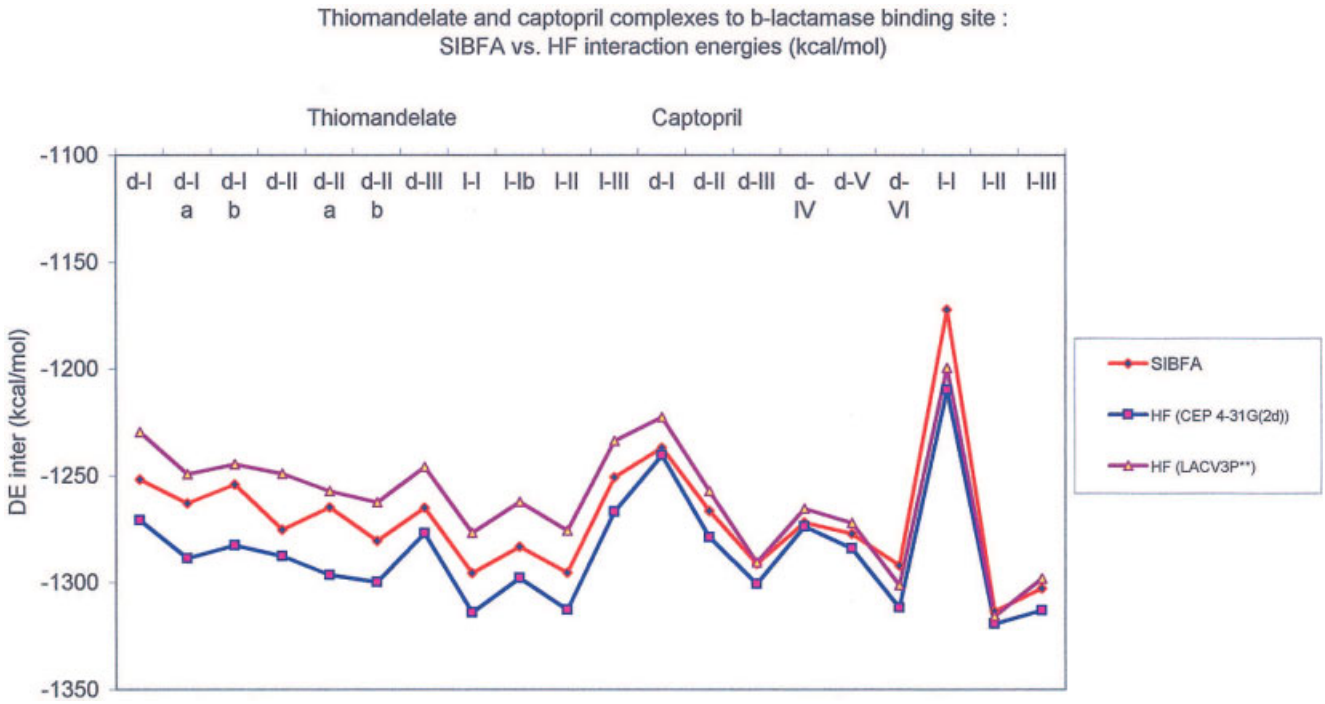

Figure 2. Evolution of ΔE(SIBFA*) and ΔE(HF)[a], and ΔE(HF)[b] in the complexes of thiomandelate and captopril with the Zn(II) cations and the fragments of the eight residues modeling the metallo-β-lactamase binding site.

$$\underset{0.0}{\text{l-I}} \approx \underset{0.2}{\text{l-II}} > \underset{12.5}{\text{l-Ib}} > \underset{15.1}{\text{d-IIb}} > \underset{20.4}{\text{d-II}} > \underset{30.7}{\text{d-III}} = \underset{30.9}{\text{d-IIa}} > \underset{32.7}{\text{d-Ia}} > \underset{41.5}{\text{d-Ib}} > \underset{43.8}{\text{d-I}} > \underset{44.9}{\text{l-III}}$$

ΔE(SIBFA*) gives the best bound complexes as being l-I and l-II, consistent with ΔE(HF) with either basis set. It gives the next two complexes as being l-Ib and d-IIb. An inversion in the relative stabilities of the next two complexes, l-Ib and d-IIb, is found, but involves 2.5 kcal/mol out of 1275, compared to ΔE(HF)[b] that gives d-IIb as more stable than l-Ib by 2 kcal/mol, while the corresponding ΔE(HF)[a] values are virtually equal. A graph displaying the evolutions of the ΔE(HF) and ΔE(SIBFA*) values (Table 2) for both thiomandelate and captopril (see below) complexes and as a function of their numbering is given in Figure 2. A more detailed analysis of the trends of the other conformers is given in Supporting Information S2. The $\delta\Delta E$ values derived from ΔE(SIBFA) are similar to those from ΔE(SIBFA*), except for d-IIb, which gives a less good agreement (3.2 kcal/mol as compared to 15.1, the corresponding HF values being 14.1). The most notable ΔE(SIBFA) deviation again concerns d-IIa, with a similar $\delta\Delta E$ as from ΔE(SIBFA*).

The values of thiomandelate conformational energy variations, δE_{thi}, are overestimated by SIBFA. Notably, a very steep increase of δE_{thi} (18.2 kcal/mol compared to 4.8 and 6.5 from HF computations) occurs for complex d-IIb, where the S^- and one O^- atoms eclipse one another at a short distance ($d_{O\text{-}S}$ = 2.92 Å) to simultaneously bind Zn(II)[b]. The overestimation of δE_{lig}(SIBFA) compared to δE_{lig}(HF) was previously noted in the case of captopril.[16] We have previously shown[32] that E_{pen} has a very pronounced attractive character when two electron-rich atoms come close together. It thus appears that its inclusion in its present formulation does not contribute to δE_{thi} lowering, because its value in the original SIBFA formulation is 16.1 kcal/mol. Further refinements in E_{pen} calibration, including a dependence of the overlap-dependent term upon atomic electron populations (as for E_{rep}) are underway and will be reported elsewhere.

The values of δE(SIBFA*) are generally close to their δE(HF)[b] counterparts. The largest deviations are for d-IIa, due to its relatively more underestimated ΔE_{int} value.

The δE evolutions are illustrated on Figure S1. This graph reflects the main features of that from Figure 2, with, however, d-IIb raised in the SIBFA graph due to its overestimated δE_{thi} term.

Correlated Computations

The results are reported in Table 3. A detailed discussion is given as Supporting Information S3. With basis set a, we observe ΔE(DFT) and ΔE(LMP2) to display exactly the same trends. With basis set b, MP2 results into a greater stabilization than DFT, ranging from 45.9

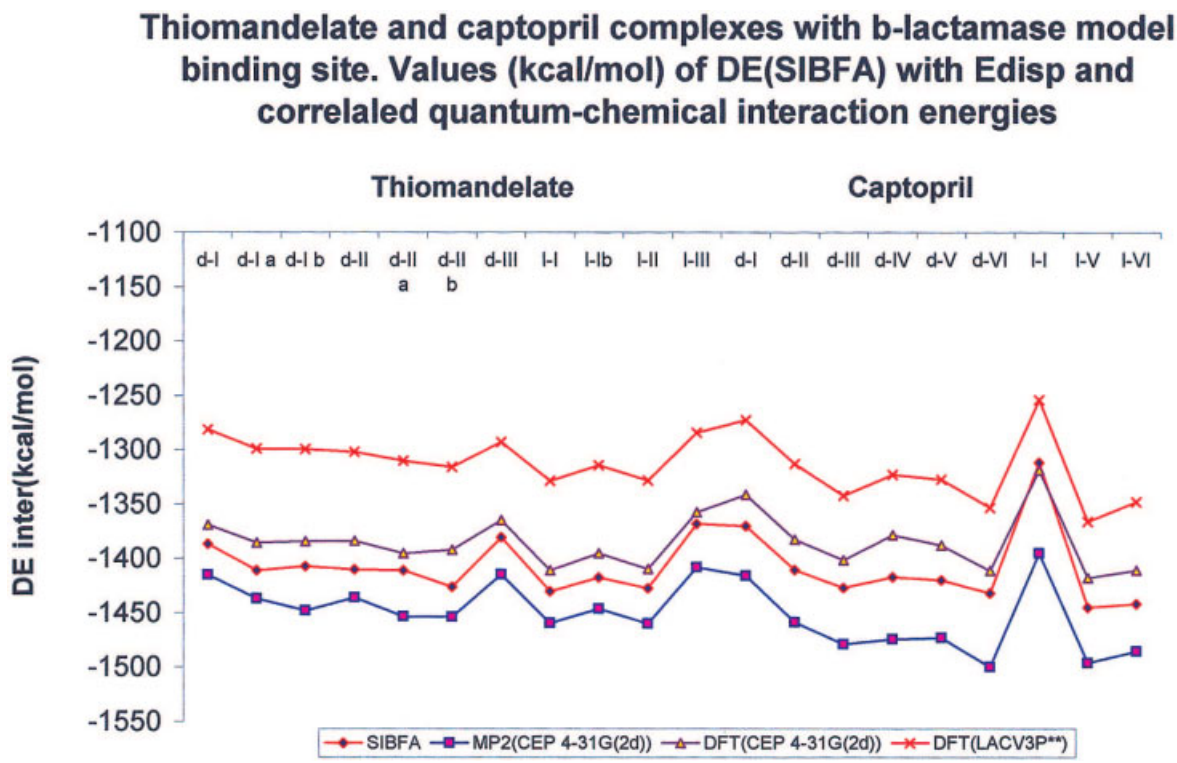

Figure 3. Evolution of ΔE_{tot}(SIBFA*) and ΔE(DFT), and ΔE(MP2)[b] in the complexes of thiomandelate and captopril with the Zn(II) cations and the fragments of the eight residues modeling the metallo-β-lactamase binding site. [Color figure can be viewed in the online issue, which is available at www.interscience.wiley.com.]

to 63.4 kcal/mol. The values of ΔE_{tot}(SIBFA*) are consistently intermediate between the ΔE(MP2) and the ΔE(DFT) ones. They are underestimated with respect to the MP2 calculations by larger but slightly more uniform amounts than at the HF level, with relative errors of 2–3%. They are overestimated with respect to the DFT computations by less uniform amounts, corresponding to relative errors of 0.5–3%. The evolutions of ΔE_{tot}(SIBFA*) and its correlated QC counterparts are represented in Figure 3. The bump in the uncorrelated ΔE(SIBFA*) graph (Fig. 2) in the d-Ib–d-IIa zone is now smoothened, but this improved agreement is probably fortuitous. The trends in ΔE_{tot}(SIBFA) are the same as those of ΔE_{tot}(SIBFA*) (not shown).

Continuum Solvation Calculations

Because of the essential role of ΔG_{solv} in the energy balances, it was important to evaluate the extent to which the trends derived from the Langlet–Claverie (LC) procedure can reproduce those from QC calculations. This evaluation was accordingly done on the 11 model thiomandelate complexes. Similar evaluations were recently reported in studies devoted to the complexes of Zn(II) with Zn-finger models,[41] and those of pentahydrated Zn(II) complexes with guanosine mononucleotide.[40a] We have reported in Table 4 the values of ΔG_{solv}(LC) along with those computed using the Poisson–Boltzmann equation within the HF and DFT procedures and the LACV3P** basis set, denoted as ΔG_{solv}(PB/HF) and ΔG_{solv}(PB/DFT), respectively. The values in the nine captopril complexes (to be commented below) are also given in this table. The graphs representing the evolutions of ΔG_{solv} are represented in Figure 4. ΔG_{solv}(LC) is seen to reproduce the trends of its QC counterparts. It has a better numerical agreement with the HF calculations than the DFT ones. The largest and smallest numerical errors with respect to ΔG_{solv}(PB/HF) are 11.6 and 1.7 kcal/mol, which amount to 6.5 and 1%, respectively. With respect to ΔG_{solv}(PB/DFT), the corresponding errors are 20.1 and 6.6 kcal/mol, amounting to 14 and 4%, respectively. In our previous study that bore on Zn-finger models,[41] relative errors of the same amplitude were also found with respect to ΔG_{solv}(PB/DFT) calculations, although the trends were consistent for the investigated Zn-finger conformers. Significantly smaller deviations were found, on the other hand, in the case of the guanine mononucleotide complexes,[40a] possibly due to the greater shielding of pentahydrated Zn(II) in these complexes than in the present ones and in the Zn-finger models.

Trends in the Individual Energy Contributions

We have reported in Table S1 the values of ΔE_{tot}(SIBFA*) and its individual components for thiomandelate and captopril. As in the 104-residue model, small energy differences between different

Table 4. Complexes of D- and L-Thiomandelate and of D- and L-Captopril with the Two Zn(II) Cations and the Eight Fragments Modeling the β-Lactamase Binding Site.

	D-thiomandelate							L-thiomandelate			
	d-I	d-Ia	d-Ib	d-II	d-IIa	d-IIb	d-III	l-I	l-Ib	l-II	l-III
ΔG_{solv}	−176.3	−150.3	−141.5	−155.9	−132.1	−137.0	−175.1	−134.4	−142.5	−137.0	−178.4
ΔG_{solv}(PB/HF)	−178.0	−141.4	−129.9	−162.3	−133.1	−138.3	−181.8	−128.5	−133.9	−131.1	−185.5
ΔG_{solv}(PB/DFT)	−163.8	−129.2	−118.0	−149.3	−120.5	−126.3	−168.3	−117.2	−122.4	−119.6	−170.6

	D-captopril						L-captopril		
	d-I	d-II	d-III	d-IV	d-V	d-VI	l-I	l-V	l-VI
ΔG_{solv}	−205.6	−150.4	−144.9	−138.6	−146.9	−141.3	−185.6	−144.5	−146.5
ΔG_{solv}(PB/HF)	−196.2	−146.4	−135.4	−139.0	−144.8	−133.4	−187.4	−126.5	−134.4
ΔG_{solv}(PB/DFT)	−177.8	−130.9	−121.4	−124.3	−129.6	−119.6	−169.4	−114.3	−122.0

Values (kcal/mol) of the solvation energies using the Langlet–Claverie Continuum reaction field model and the Poisson–Boltzmann equation in quantum-chemical computations.

complexes can result in several cases from compensations between large energy differences of individual components. This is particularly striking upon comparing complexes d-IIb and l-II, which have virtually identical ΔE_{tot} values, of −1426.1.0 and −1427.6 kcal/mol. d-IIb is the complex having both the lowest E_1 value and the highest sum of $E_{pol} + E_{ct}$. Although it is favored over l-II by 25.3 kcal/mol in terms of E_1, and by 1.4 and 13.4 kcal/mol in terms of E_{ct} and E_{disp}, it is disfavored with respect to it by 41.2 kcal/mol in terms of E_{pol}.

Captopril

We have previously reported the analysis of captopril binding to β-lactamase in nine distinct complexes, validated by parallel computations on the model binding sites.[16] Although the trends from SIBFA were consistent with the QC ones, the ΔE(SIBFA) values were underestimated with respect to the ΔE(HF) ones, due to an exaggerated anticooperative character of E_{ct}(SIBFA). We have accordingly recomputed the interaction energies with the modified

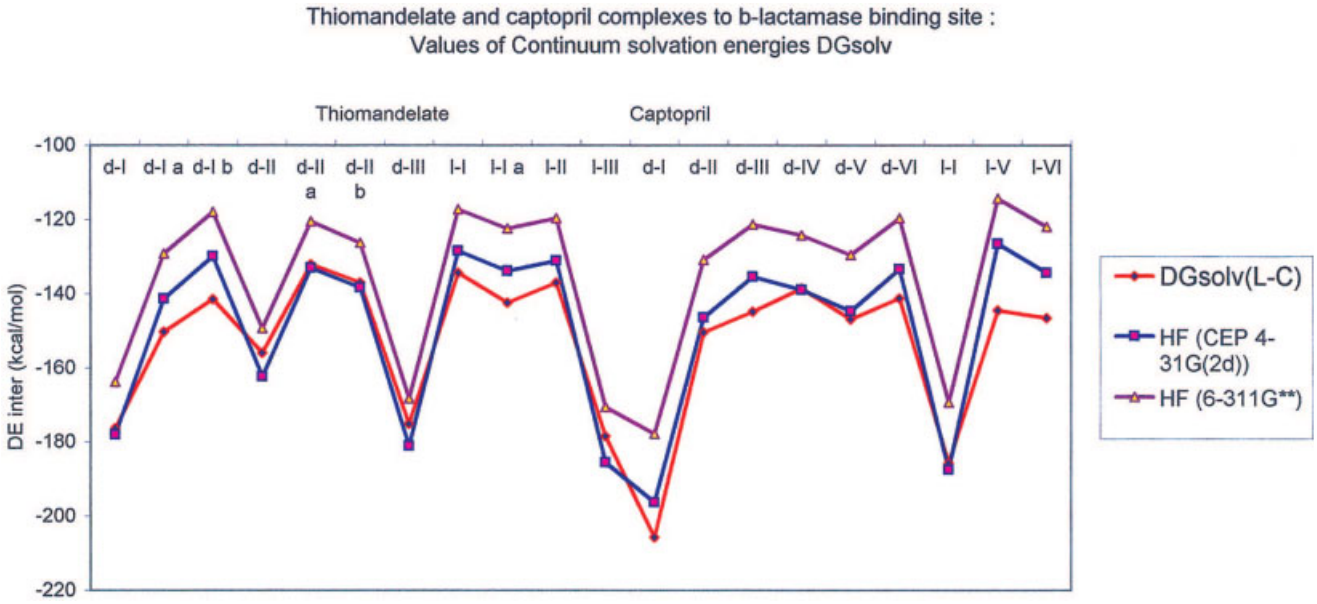

Figure 4. Evolution of ΔG_{solv}(LC) and ΔG_{solv}(PB/HF) and ΔG_{solv}(PB/DFT) in the thiomandelate and captopril with the Zn(II) cations and the fragments of the eight residues modeling the metallo-β-lactamase binding site. [Color figure can be viewed in the online issue, which is available at www.interscience.wiley.com.]

Table 5. Complexes of D- and L-Captopril with the Two Zn(II) Cations and the Eight Fragments Modeling the β-Lactamase Binding Site.

	D-captopril						L-captopril		
	d-I	d-II	d-III	d-IV	d-V	d-VI	l-I	l-V	l-VI
ΔE(HF)[a]	**−1222.6**	**−1257.2**	**−1290.5**	**−1265.4**	**−1272.0**	**−1301.2**	**−1199.6**	**−1315.7**	**−1298.0**
$\delta\Delta E$	93.1	58.5	25.2	50.3	43.7	14.5	116.1	0.0	17.7
ΔE(HF)[b]	**−1240.3**	**−1278.8**	**−1300.5**	**−1273.8**	**−1284.0**	**−1311.6**	**−1209.8**	**−1319.2**	**−1313.0**
$\delta\Delta E$	78.9	40.4	18.7	45.4	35.2	8.6	109.4	0.0	6.2
ΔE(SIBFA)	**−1217.6**	**−1248.9**	**−1273.2**	**−1255.7**	**−1259.3**	**−1273.1**	**−1186.3**	**−1296.7**	**−1281.4**
$\delta\Delta E$	79.1	47.8	23.5	41.0	37.4	23.6	110.4	0.0	15.3
ΔE(SIBFA*)	**−1236.8**	**−1266.4**	**−1291.2**	**−1271.8**	**−1277.0**	**−1291.9**	**−1172.4**	**−1313.3**	**−1302.6**
$\delta\Delta E$*	76.5	46.9	22.1	41.5	36.3	21.4	140.9	0.0	10.7
$\delta(\Delta E$(SIBFA*)/ΔE(HF)[a])	−14.2	−9.2	−0.7	−6.4	−5.0	9.3	27.2	−2.4	−4.6
$\delta(\Delta E$(SIBFA*)/ΔE(HF))[b]	3.5	12.4	9.3	2.0	7.0	19.7	37.4	5.9	10.4

Values (kcal/mol) of the intermolecular interaction energies. Uncorrelated calculations and SIBFA ΔE values without the dispersion contribution.
[a]LACV3P** basis set.
[b]CEP(4-31G(2d)) basis set.

Zn-specific E_{ct} calibration and modified imidazole and thiomandelate screening parameters and resorted to the two SIBFA E_1 formulations. The comparisons with uncorrelated and correlated QC computations are reported in Tables 5 and 6, respectively. The computations bear on six D-captopril and three L-captopril complexes, as described in detail in ref. 16. Briefly, d-I–d-III are monodentate complexes, in which S^- bridges the two Zn cations, with the carboxylate and carbonyl in complexes d-II and d-III interacting with the Lys184 and Asn193 residues. d-IV–d-VI are bidentate complexes, with the additional involvement of the carbonyl group to Zn(II)[b] binding for d-IV and d-V, and of that of one carboxylate O^- in d-VI. l-I is monodentate, with the carbonyl group H-bonded to the Asn main-chain N, and d-V and d-VI are bidentate with the additional involvement of the carbonyl in Zn(II)[b] binding. Recently, Garcia–Saez et al. have published the X-ray diffraction structure of the complex of D-captopril with the metallo-β-lactamase from *C. meningosepticum*.[45] Although D-captopril does bind with S^- bridging monodentately the two Zn(II)

Table 6. Complexes of D- and L-Captopril with the Two Zn(II) Cations and the Eight Fragments Modeling the β-Lactamase Binding Site.

	D-captopril						L-captopril		
	d-I	d-II	d-III	d-IV	d-V	d-VI	l-I	l-V	l-VI
LACV3P** basis set									
ΔE(DFT)	−1272.8	−1313.0	−1342.1	−1323.1	−1327.6	−1353.2	−1254.3	−1366.1	−1348.0
ΔE(LMP2)	−1264.4	−1307.1	−1332.6	−1309.4	−1316.2	−1337.4	−1246.0	−1348.2	−1331.5
CEP4-31G(2d) basis set									
ΔE(DFT)	**−1341.4**	**−1382.5**	**−1401.6**	**−1378.4**	**−1388.0**	**−1411.5**	**−1319.0**	**−1417.8**	**−1410.9**
$\delta\Delta E$	76.4	35.3	16.2	39.4	29.8	6.2	98.8	0.0	6.9
ΔE(MP2)	**−1415.9**	**−1458.8**	**−1478.8**	**−1474.3**	**−1473.1**	**−1500.0**	**−1395.4**	**−1496.3**	**−1485.6**
$\delta\Delta E$	80.4	37.5	17.5	22.0	23.2	−3.7	100.9	0.0	10.7
ΔE_{tot}(SIBFA*)	**−1370.1**	**−1410.7**	**−1427.1**	**−1417.0**	**−1419.9**	**−1431.8**	**−1311.8**	**−1445.2**	**−1441.7**
$\delta\Delta E$*	75.1	34.5	18.1	28.2	25.3	13.4	133.4	0.0	3.5
$\delta(\Delta E_{tot}$(SIBFA*)/ ΔE(DFT)[b])	−28.7	−28.2	−25.5	−38.6	−31.9	−20.3	7.2	−27.4	−30.8
$\delta(\Delta E_{tot}$(SIBFA*)/ ΔE(EMP2[b])	45.8	48.1	51.7	57.3	53.2	68.2	83.6	51.1	43.9

Values (kcal/mol) of the intermolecular interaction energies. Correlated calculations and SIBFA ΔE values with the dispersion contribution.
[a]LACV3P** basis set.
[b]CEP (4-31G(2d)) basis set.

cations, the conformation of the complex is not superimposable on complex d-II. This could be due to differences in the nature of some of the residues in the active sites of the metallo-β-lactamases of *C. meningosepticum* and *B. fragilis.* The most important difference relates to Lys167 of the former, which is involved in an ionic bond with the carboxylate, and is replaced by an aliphatic residue, Leu133, in the homologous position in *B. fragilis* β-lactamase. This could orient the D-captopril carboxylate to bind to the nearest cationic residue in *B. fragilis* β-lactamase, namely Lys184.

Uncorrelated QC Results

Table 5 shows an improved numerical agreement of ΔE(SIBFA) with $\Delta E(\mathrm{HF})^{b}$ compared to the values reported in ref. 16, and a further improved numerical agreement of ΔE(SIBFA*) with it. ΔE(SIBFA*) is underestimated with respect to $\Delta E(\mathrm{HF})^{b}$ by values in the range of 2.3–35.2 out of 1210 kcal/mol, corresponding to relative errors in a 0–3% range. The differences with respect to the $\Delta E(\mathrm{HF})^{a}$ energies are in the range -15.4–25.0 kcal/mol, which corresponds to relative errors in the 1–2% range. The energy ranking of the nine complexes is as follows:

$$\delta\Delta E(\mathrm{HF})^{a}$$

$$\underset{0.0}{\text{l-V}} > \underset{14.5}{\text{d-VI}} \geq \underset{17.7}{\text{l-VI}} > \underset{25.2}{\text{d-III}} > \underset{43.7}{\text{d-V}} > \underset{50.3}{\text{d-IV}} > \underset{58.5}{\text{d-II}} > \underset{93.1}{\text{d-I}} > \underset{116.1}{\text{l-I}}$$

$$\delta\Delta E(\mathrm{HF})^{b}$$

$$\underset{0.0}{\text{l-V}} > \underset{6.2}{\text{l-VI}} \geq \underset{8.6}{\text{d-VI}} > \underset{18.7}{\text{d-III}} > \underset{35.2}{\text{d-V}} > \underset{40.4}{\text{d-II}} > \underset{45.4}{\text{d-IV}} > \underset{78.9}{\text{d-I}} > \underset{109.4}{\text{l-I}}$$

$$\delta\Delta E(\mathrm{SIBFA}^{*})$$

$$\underset{0.0}{\text{l-V}} > \underset{10.7}{\text{l-VI}} > \underset{21.4}{\text{d-VI}} \approx \underset{22.1}{\text{d-III}} > \underset{36.3}{\text{d-V}} > \underset{41.5}{\text{d-IV}} > \underset{46.9}{\text{d-II}} > \underset{76.5}{\text{d-I}} > \underset{140.9}{\text{l-I}}$$

The $\delta\Delta E$(SIBFA*) ranking is the same as the $\delta\Delta E(\mathrm{HF})^{b}$ one except for an interchange of d-II and d-IV, in keeping with our previous results,[16] but this interchange also occurs with $\delta\Delta E(\mathrm{HF})^{a}$. We had then noted the inversion of relative energies of d-VI and l-VI in the HF^{a} vs. HF^{b} computations, but these involve small energy differences of <3.2 kcal/mol out of 1300, while the relative SIBFA* destabilization of d-VI compared to l-VI, although consistent with $\Delta E(\mathrm{HF})^{b}$, involves a larger amount of 10.7 kcal/mol. The other complex with a large relative ΔE(SIBFA*) vs. $\Delta E(\mathrm{HF})^{b}$ error (3%) is l-I, the highest lying complex in the series. This could be due to a shortening in the carbonyl O to Asn193 main chain N distance (2.65 Å), translated in steeper increases in E_{rep}(SIBFA) than E_{exch}(HF).

Correlated QC Calculations

The results are commented in detail in Supporting Information 4. Table 6 shows $\Delta E(\mathrm{MP2})^{b}$ to have larger magnitudes than $\Delta E(\mathrm{DFT})^{b}$, consistent with the thiomandelate results, and ΔE_{tot}(SIBFA*) to have values intermediate between the MP2 and DFT ones, except for complex l-I. The graphs comparing the evolutions of ΔE(SIBFA*) and ΔE_{tot}(SIBFA*) and their QC counterparts regrouped with the thiomandelate ones are displayed in Figures 2 and 3, showing the good parallelism of the curves.

Continuum Solvation Energies

The values of ΔG_{solv}(LC) are generally consistent with their ΔG_{solv}(PB/DFT) and ΔG_{solv}(PB/HF) counterparts, as seen from Table 4 and Figure 4, except for complex l-V, with the least ΔE_{solv} value, for which the relative error has raised to 26 and 14%, respectively. For the eight other complexes, it is in the ranges of 10–19% and 0–9%, respectively.

Trends in the Individual Energy Contributions

Examination of the trends of the individual contributions of ΔE_{tot}(SIBFA*) (Table S1) again shows that for some complexes, relatively small energy differences can result from compensations between large energy differences. One example is that of the monodentate d-III complex compared to the bidentate d-VI one. These two complexes have ΔE_{tot} values differing by 4.7 kcal/mol out of 1430, that is, 0.5%. Although d-III is disfavored by 49.5 and 4 kcal/mol with respect to d-VI in terms of E_{l} and E_{disp}, respectively, it is favored over it by 52.2 and 1 kcal/mol in terms of E_{pol} and E_{ct}, respectively.

Conclusions and Perspectives

The energy balances on the 104-residue model of β-lactamase on 11 energy-minimized thiomandelate complexes showed the D-isomer to have a greater affinity than the L one, the best binding mode, d-I, having the S^{-} bridging monodentately the two Zn(II) cations, and one carboxylate O^{-} H-bonded to the Asn193 side chain. In this connection, previous energy balances for captopril binding had also found the D-isomer to have a larger affinity than the L one, and showed that in the most stable binding mode, while S^{-} was also monodentately bridging the two Zn(II) cations, the carboxylate was simultaneously bound to the Lys184 side chain and to the Asn193 main chain.[16] Although such a model was fully consistent with an X-ray crystal diffraction study on the complex of a mercaptocarboxylate inhibitor, with a related metallo-β-lactamase to that of *B. fragilis,* namely *P. aeruginosa,*[6] there are no X-ray studies on thiomandelate complexes. The fact that in the best thiomandelate complex, the carboxylate is bound to the side chain rather than the main chain of Asn193 and cannot reach out to make an ionic bond with Lys184 may reflect the smaller size of thiomandelate than captopril, with only one C atom in-between the thiolate and carboxylate groups instead of four C and one N atoms in the case of captopril. Despite the small size of thiomandelate, several alternative, competing, modes of binding were found. Several of these retained the monodentate S^{-} Zn(II)-bridging mode, while the carboxylate could bind to either Lys184, or to either the Asn193 main-chain N or the side-chain N. The only case of simultaneous interaction of the carboxylate with both residues was complex d-Ib, which involved both side chains. We have also characterized bidentate binding modes, namely d-II and d-IIb, in which one carboxylate O^{-} partakes in $\mathrm{Zn(II)}^{b}$ binding. Although such complexes have among the most stabilizing interaction ener-

gies in the model sites, their E_{tot} values become equilibrated with those of the other complexes in the 104-residue model, with further loss in relative stabilities with respect to some monodentate complexes due to ΔG_{solv}. A reservation to the present treatment is the absence of residues Gly48 and Trp49, which belong to a flexible loop that because of its thermal disorder, could not be characterized by X-ray diffraction of the native enzyme,[5] but was reported to be involved in ligand binding.[46] As mentioned in ref. 16, such residues could partly shield the cavity from the solvent, thereby affecting the relative ΔG_{solv} values in the competing arrangements, while possibly contributing additional stabilization to inhibitor binding in some of these. For each captopril complex, 100 ps molecular dynamics using the classical CFF91 potential and $Zn–S^-/O^-$ distance restraints that differ according to the nature of each considered complex have identified several frames with varying loop locations but closely similar energies (Antony and Gresh, unpublished). Each candidate low-energy frame should be used as a starting point and postprocessed by SIBFA energy minimization in the presence of continuum solvation, with a similar treatment applied for the thiomandelate complexes. This is beyond the scope of the present study.

An essential goal of this work was an objective evaluation of the accuracy of the SIBFA procedure for complexes of flexible molecules in metalloenzyme binding sites. As in ref. 16, this was done by performing parallel SIBFA and *ab initio* computations on the thiomandelate complexes with the eight β-lactamase residues of the recognition site. Two different basis sets were used, and we have carried out uncorrelated HF as well as correlated DFT, LMP2, and MP2 QC computations. This evaluation was extended to the nine captopril complexes previously investigated,[16] now resorting to the modified Zn-E_{ct}, the modified methanethiolate and imidazole E_{pol} calibration, as well as testing the new formulation of E_{MTP} and E_{rep}, thereby totalling 20 different complexes. ΔE(SIBFA*) was found to have values close to, and generally intermediate between, ΔE(HF) using the LACV3P** (a) and the CEP 4-31G(2d) (b) basis sets, as seen from Figure 2. It reproduced ΔE(HF) from these sets with relative errors in the ranges of 1–2% for set (a) and 1–3% for set (b). These agreements are noteworthy considering: (a) the very large magnitudes of ΔE; (b) the presence of two dicationic charges close to one another ($d_{Zn\text{-}Zn}$ = 3.5 Å) and that of two ligand anionic charges that can be brought into vicinity upon cation binding, both proximities translating into very large nonadditivity effects; (c) the need to compute in simultaneous and consistent fashion intra- and intermolecular polarization and charge-transfer contributions; (d) the competition between mono- vs. bidentate S^- binding to Zn(II) and that between the carboxylate bound by an ionic H-bond to Lys184 vs. a polar H-bond to Asn193; (e) the fact that small ΔE(SIBFA*) energy differences stem from large and mutually compensating differences at the level of individual contributions. Some complexes differed by app. 1% in their ΔE values, that is, less than the actual accuracy in ΔE(SIBFA*). This has resulted only in few cases into SIBFA inverting the ranking found in ΔE(HF), as for d-II compared to d-IIa. A more uniform agreement was obtained between ΔE_{tot}(SIBFA*) and its correlated counterparts ΔE(DFT) and ΔE(MP2) with basis set b, as illustrated in Figure 3, particularly ΔE(MP2), even though the largest relative error (6% for the least stably bound captopril complex l-I) was larger than with respect to ΔE(DFT) (2.5%). Such an apparent parallelism is noteworthy, considering that in the present treatment, correlation/dispersion effects were introduced in SIBFA only through the addition of E_{disp} contribution, resorting to the same uncorrelated multipoles and polarizabilities as for ΔE(SIBFA*). The recalibration of SIBFA on the basis of correlated energy decomposition and using correlated multipoles and polarizabilities is underway (Piquemal et al., unpublished results). The results of this calibration for peptides will be reported in a forthcoming article. The present study builds up on the results of several previously reported validation studies of the SIBFA procedure with respect to numerous QC calculations. These bore on polycoordinated complexes of divalent cations,[37,40,47] multiply H-bonded complexes,[48] conformational studies of flexible molecules,[18d] and the issue of multipole transferability.[18] As in the present study, the values of ΔE_{int} were found to persistently match their QC counterparts with relative errors $<3\%$. The present refinements to E_{MTP} and E_{rep} were themselves tested and validated in the accompanying article for several polycoordinated, mono-, as well as binuclear Zn(II) complexes. Presently, two shortcomings of SIBFA could be observed. The first related to the values of thiomandelate conformational energy variations δE_{thi}, which compared less favorably to their QC counterparts, as they were overestimated at the shorter (<3.0 Å) $S^-–O^-$ intramolecular distances. Further refinements of E_{pen} could possibly more efficiently counteract the ligand–ligand electrostatic and repulsion contributions for such distances. The second related to continuum solvation energy. Thus, although ΔG_{solv}(LC) was able to reproduce the trends of its QC counterparts, ΔG_{solv}(PB/HF) and ΔG_{solv}(PB/DFT) (Fig. 4), the relative errors were larger than the corresponding ΔE(SIBFA*) ones, and significantly accented for one complex, captopril l-V, namely 14 and 26% with respect to the two approaches. For the remaining nineteen complexes, it was in the ranges 0.3–9% and 4–19%, respectively. Larger magnitudes of ΔG_{solv}(LC) than ΔG_{solv}(PB/DFT) were previously noted in cases where a Zn(II) dication is partly exposed to the solvent even though a correct ordering in ΔG_{solv}(PB/DFT) obtained with ΔG_{solv}(LC).[41] Further refinements in the expression of ΔG_{solv} could be necessary to avoid an imbalance of ΔE_{int} and ΔG_{solv} effects within δE_{fin}. One of these consists into iteratively including the contributions to the solute electrostatic potential of the dipoles induced on it by the reaction field of the solvent (Langlet et al., unpublished).

Finally, the present validation tests could be used to benchmark other polarizable molecular mechanics as well. Therefore, we provide as Supporting Information the pdb files of all 20 complexes of thiomandelate and captopril with the β-lactamase binding site. They are also posted on the Web site at http://www.lct.jussieu.fr/jpp/SIBFA.html.

Acknowledgments

The *ab initio* computations were performed on the computers of the Centre d'Informatique National de l'Enseignement Supérieur (CINES, Montpellier, France), of the Centre de Ressources Informatiques de Haute Normandie (CRIHAN, Rouen, France), and of the Institut de Developpement en Ressources Informatiques (ID-

RIS, Orsay, France). We wish to thank Nicole Audiffren (CINES) for her help in the large-scale MP2 computations.

Supporting Information

Supporting Information S1. Trends of the individual energy contributions in the complexes of thiomandelate with the 104-residue model of β-lactamase. **Supporting Information S2.** Complexes of thiomandelate with the two Zn(II) cations and the eight fragments modeling the metallo-β-lactamase binding site. Uncorrelated computations. **Supporting Information S3.** Complexes of thiomandelate with the two Zn(II) cations and the eight fragments modeling the metallo-β-lactamase binding site. Correlated computations. **Supporting Information S4.** Complexes of captopril with the two Zn(II) cations and the eight fragments modeling the metallo-β-lactamase binding site. Correlated QC calculations. **Table S1.** Complexes of metallo-β-lactamase binding site with thiomandelate and captopril. Values of ΔE_{tot}(SIBFA*) and of its individual contributions. **Figure S1.** Evolution of δE(SIBFA*) and $\delta E(\mathrm{HF})^a$ and $\delta E(\mathrm{HF})^b$ in the complexes of metallo-β-lactamase binding site with thiomandelate and captopril.

Additional Supporting Information

Structures in pdb format of the complexes of thiomandelate and captopril with the β-lactamase recognition site.

References

1. Cricco, J. A.; Orellano, E. G.; Rasia, R. M.; Vila, A. J. Coord Chem Rev 1999, 190–192, 519.
2. Wang, Z.; Fast, W.; Valentine, A. M.; Benkovic, S. J. Curr Opin Chem Biol 1999, 3, 614.
3. (a) Salsbury, F. R., Jr.; Crowly, M. F.; Brooks, C. L., III. Proteins 2001, 44, 448; (b) Suarez, D.; Merz, K. M., Jr. J Am Chem Soc 2001, 123, 3759; (c) Diaz, N.; Suarez, D.; Merz, K. M., Jr. J Am Chem Soc 2001, 123, 9867; (d) Suarez, D.; Brothers, E. N.; Merz, K. M., Jr. Biochemistry 2002, 41, 6615; (e) Suarez, D.; Diaz, N.; Merz, K. M., Jr. J Comput Chem 2002, 23, 1587; (f) Oelschlaeger, P.; Schmid, R. D.; Pleiss, J. Protein Eng 2003, 16, 341; (g) Oelschlaeger, P.; Schmid, R. D.; Pleiss, J. Biochemistry 2003, 42, 8945; (h) Dal Peraro, M.; Vila, A. J.; Carloni, P. Proteins 2004, 54, 412.
4. (a) Gilson, H. S. R.; Krauss, M. J Am Chem Soc 1999, 121, 6984; (b) Diaz, N.; Suarez, D.; Merz, K. M., Jr. J Am Chem Soc 2000, 122, 4197; (c) Krauss, M.; Gilson, H. S. R.; Gresh, N. J Phys Chem B 2001, 105, 8040; (d) Olsen, L.; Antony, J.; Hemmingsen, L.; Mikkelsen, K. J Phys Chem A 2002, 106, 1046; (e) Dal Peraro, M.; Vila, A. J.; Carloni, P. J Biol Inorg Chem 2002, 7, 704; (f) Krauss, M.; Gresh, N.; Antony, J. J Phys Chem B 2003, 108, 1215; (g) Olsen, L.; Antony, J.; Ryde, U.; Adolph, H.-W.; Hemmingsen, L. J Phys Chem B 2003, 107, 2366; (h) Dal Peraro, M.; Vila, A. J.; Carloni, P. Inorg Chem 2003, 42, 45.
5. Concha, N. O.; Rasmussen, B. A.; Bush, K.; Herzberg, O. Structure 1996, 4, 823.
6. Concha, N. O.; Janson, P. A.; Rowling, P.; Pearson, S.; Cheaver, C. A.; Clarke, B. P.; Lewis, C.; Galleni, M.; Frère, J.-M.; Payne, D. J.; Bateson, J. H.; Abdel–Meguid, S. S. Biochemistry 2000, 39, 4288.
7. Garcia–Saez, I.; Mercuri, P. S.; Papamicael, C.; Kahn, R.; Frère, J.-M.; Galleni, M.; Rossolini, G. M.; Dideberg, O. J Mol Biol 2003, 325, 651.
8. (a) Carfi, A.; Pares, S.; Duee, E.; Galleni, M.; Duez, C.; Frere, J.-M.; Dideberg, O. EMBO J 1995, 14, 4914. (b) Carfi, A.; Duee, E.; Paul–Soto, R.; Galleni, M.; Frère, J.-M.; Dideberg, O. Acta Crystallogr D 1998, 54, 47.
9. Fabiane, S. M.; Sohi, M. K.; Wan, T.; Payne, D. J.; Bateson, J. H.; Mitchell, T.; Sutton, B. J. Biochemistry 1998, 37, 12404.
10. Toney, J. H.; Fitzgerald, P. M. D.; Grover–Sharma, N.; Olson, S. H.; May, W. H.; Sundelof, J. G.; Vanderwall, D. E.; Cleary, K. A.; Grant, S. K.; Wu, J. K.; Kozarich, J. W.; Pompliano, D. L.; Hammond, G. C. Chem Biol 1998, 5, 185.
11. Ullah, J. H.; Walsh, T. R.; Taylor, I. A.; Emery, D. C.; Verma, C. S.; Gamblin, S. J.; Spencer, J. J Mol Biol 1998, 284, 125.
12. Toney, J. H.; Hammond, G. G.; Fitzgerald, P. M. D.; Sharma, N.; Balkovec, J. M.; Rouen, G. P.; Olson, S. H.; Hammond, M. L.; Greenlee, M. L.; Gao, Y.-D. J Biol Chem 2001, 276, 31913.
13. Siemann, S.; Evanoff, D. P.; Marrone, L.; Clarke, A. J.; Viswanatha, T.; Dmitrienko, G. I. Antimicrob Agents Chemother 2002, 46, 2450.
14. Damblon, C.; Jensen, M.; Ababou, A.; Barsukov, I.; Papamicael, C.; Schofield, C. J.; Olsen, L.; Bauer, R.; Roberts, G. C. K. J Biol Chem 2003, 278, 29240.
15. Mollard, C. C.; Papamicael, C.; Damblon, C.; Vessilier, S.; Amicosante, G.; Schofield, C. J.; Galleni, M.; Frère, J. M.; Roberts, G. C. K. J Biol Chem 2001, 276, 45015.
16. Antony, J.; Gresh, N.; Olsen, L.; Hemmingsen, L.; Schofield, C. S.; Bauer, R. J Comput Chem 2002, 23, 1281.
17. Faerman, C. H.; Price, S. L. J Am Chem Soc 1990, 112, 4915.
18. (a) Rogalewicz, F.; Ohanessian, G.; Gresh, N. J Comput Chem 2000, 21, 963; (b) Tiraboschi, G.; Fournie–Zaluski, M.-C.; Roques, B.-P.; Gresh, N. J Comput Chem 2001, 22, 103; (c) Gresh, N.; Shi, G.-B. J Comput Chem 2004, 25, 160; (d) Gresh, N.; Kafafi, S. A.; Truchon, J.-F.; Salahub, D. R. J Comput Chem 2004, 25, 823.
19. Ren, P.; Ponder, J. W. J Comput Chem 2002, 23, 1497.
20. Stevens, W. J.; Basch, H.; Krauss, M. J Chem Phys 1984, 81, 6026.
21. Hay, P. J.; Hadt, W. R. J Chem Phys 1985, 82, 299.
22. Pople, J. A.; Binkley, J. S.; Seeger, R. Int J Quantum Chem 1976, Symp. 10, 1.
23. (a) Lee, C.; Yang, W.; Parr, R. G. Phys Rev 1988, B37, 785; (b) Becke, A. J Chem Phys 1993, 98, 5648.
24. (a) Saebo, S.; Pulay, P. J Chem Phys 1987, 86, 914; (b) Saebo, S.; Pulay, P. J Chem Phys 1988, 88, 1884; (c) Saebo, S.; Tong, W.; Pulay, P. J Chem Phys 1993, 98, 2170.
25. Frisch, M. J.; Trucks, G. W.; Schlegel, H. B.; Scuseria, G. E.; Robb, M. A.; Cheeseman, J. R.; Montgomery, J. A., Jr.; Vreven, T.; Kudin, K. N.; Burant, J. C.; Millam, J. M.; Iyengar, S. S.; Tomasi, J.; Barone, V.; Mennucci, B.; Cossi, M.; Scalmani, G.; Rega, N.; Petersson, G. A.; Nakatsuji, H.; Hada, M.; Ehara, M.; Toyota, K.; Fukuda, R.; Hasegawa, J.; Ishida, M.; Nakajima, T.; Honda, Y.; Kitao, O.; Nakai, H.; Klene, M.; Li, X.; Knox, J. E.; Hratchian, H. P.; Cross, J. B.; Adamo, C.; Jaramillo, J.; Gomperts, R.; Stratmann, R. E.; Yazyev, O.; Austin, A. J.; Cammi, R.; Pomelli, C.; Ochterski, J. W.; Ayala, P. Y.; Morokuma, K.; Voth, G. A.; Salvador, P.; Dannenberg, J. J.; Zakrzewski, V. G.; Dapprich, S.; Daniels, A. D.; Strain, M. C.; Farkas, O.; Malick, D. K.; Rabuck, A. D.; Raghavachari, K.; Foresman, J. B.; Ortiz, J. V.; Cui, Q.; Baboul, A. G.; Clifford, S.; Cioslowski, J.; Stefanov, B. B.; Liu, G.; Liashenko, A.; Piskorz, P.; Komaromi, I.; Martin, R. L.; Fox, D. J.; Keith, T.; Al-Laham, M. A.; Peng, C. Y.; Nanayakkara, A.; Challacombe, M.; Gill, P. M. W.; Johnson, B.; Chen, W.; Wong, M. W.; Gonzalez, C.; Pople, J. A. Gaussian 03, Revision B.05; Gaussian, Inc.: Pittsburgh, PA, 2003.
26. Jaguar 5.0. Schrodinger Inc., Portland, Oregon, 2002.
27. Murphy, R. B.; Beachy, M. D.; Friesner, R. A. J Chem Phys 1995, 103, 1481.
28. Tannor, D. K.; Marten, B.; Murphy, R.; Friesner, R. A.; Sitkoff, D.;

Ringnalda, M.; Goddard, W. A., III; Honig, B. J Am Chem Soc 116, 11875.
29. Vigné–Maeder, F.; Claverie, P. J Chem Phys 1988, 88, 4934.
30. Garmer, D. R.; Stevens, W. J. J Phys Chem 1989, 93, 8263.
31. (a) Gresh, N.; Claverie, P.; Pullman, A. Int J Quantum Chem 1986, 29, 101; (b) Gresh, N. J Comput Chem 1995, 16, 856; (c) Gresh, N. J Phys Chem A 1997, 101, 8680; (d) Gresh, N.; Guo, H.; Salahub, D. R.; Roques, B.-P.; Kafafi, S. A. J Am Chem Soc 1999, 121, 7885.
32. Piquemal, J.-P.; Gresh, N.; Giessner–Prettre, C. J Phys Chem A 2003, 107, 10353.
33. Murrell, J. N.; Teixeiras–Dias, J. J. C. Mol Phys 1970, 19, 521.
34. Piquemal J. P.; Merging, A.; Parioel, O.; Giessner-Prettre, C. J Comput Chem 2005, 26, 1052.
35. Gresh, N.; Piquemal, J.-P.; Krauss, M. J Comput Chem 2005, 26, 1113.
36. Stevens, W. J.; Fink, W. Chem Phys Letts 1987, 139, 15.
37. (a) Tiraboschi, G.; Gresh, N.; Roques, B.-P. J Comput Chem 1999, 20, 1979; (b) Tiraboschi, G.; Gresh, N.; Giessner–Prettre, C.; Pedersen, L. G.; Deerfield, D. W. J Comput Chem 2000, 21, 1011.
38. Langlet, J.; Claverie, P.; Caillet, J.; Pullman, A. J Phys Chem 1988, 92, 1631.
39. Langlet, J.; Gresh, N.; Giessner–Prettre, C. Biopolymers 1995, 36, 765.
40. (a) Gresh, N.; Sponer, J. E.; Spackova, N.; Leszczynski, J.; Sponer, J. J Phys Chem B 107, 8669; (b) Ledecq, M.; Lebon, F.; Durant, F.; Giessner–Prettre, C.; Marquez, A.; Gresh, N. J Phys Chem B 2003, 107, 10640.
41. Gresh, N.; Derreumaux, P. J Phys Chem B 2003, 107, 4862.
42. Gresh, N.; Claverie, P.; Pullman, A. Theoret Chim Acta 1984, 66, 1.
43. Evangelakis, G.; Rizos, J.; Lagaris, I.; Demetropoulos, G. N. Comput Phys Commun 1987, 46, 401.
44. Force-Field Cff91. Discover Software, Accelrys Inc., San Diego, CA.
45. Garcia–Saez, I.; Hopkins, J.; Papamicael, C.; Franceschini, N.; Amicosante, G.; Rossolini, G. M.; Galleni, M.; Frere, J.-M.; Dideberg, O. J Biol Chem 2003, 26, 23868.
46. (a) Scrofani, S. D.; Chung, J.; Huntley, J. J.; Benkovic, S. J.; Wright, P. E.; Dyson, H. J. Biochemistry 1999, 38, 14507; (b) Huntley, J. J.; Scrofani, S. D.; Osborne, M. J.; Wright, P. E.; Dyson, H. J. Biochemistry 2000, 39, 13356; (c) Moali, C.; Anne, C.; Lamotte–Brasseur, J.; Groslambert, S.; Devreese, B.; Van Beeumen, J.; Galleni, M.; Frere, J.-M. Chem Biol 2003, 10, 319; (d) Huntley, J. J.; Fast, W.; Benkovic, S. J.; Wright, P. E.; Dyson, H. J. Protein Sci 2003, 12, 1368.
47. Garmer, D. R.; Gresh, N.; Roques, B.-P. Proteins 1998, 31, 42.
48. (a) Gresh, N. J Phys Chem A 1997, 8680; Masella, M.; Gresh, N.; Flament, J.-P. J Chem Soc Faraday Trans 1998, 94, 2745.